

## Research Article

# Experimental Study on Crushing Characteristics of Lignite under Different Load Conditions

Ziwen Dong <sup>1,2</sup>

<sup>1</sup>*School of Safety Engineering, Ningbo University of Technology, Ningbo, Zhejiang 315211, China*

<sup>2</sup>*Zhejiang Institute of Tianjin University, Ningbo, Zhejiang 315211, China*

Correspondence should be addressed to Ziwen Dong; 1316859454@qq.com

Received 31 March 2022; Accepted 2 June 2022; Published 17 June 2022

Academic Editor: Ramadhansyah Putra Jaya

Copyright © 2022 Ziwen Dong. This is an open access article distributed under the Creative Commons Attribution License, which permits unrestricted use, distribution, and reproduction in any medium, provided the original work is properly cited.

Coal particle size and the degree of compaction significantly affect the goaf heritage ventilated environment and the process of spontaneous combustion of coal, the distribution of particle size and compaction degree are also affected by the load size and the application process, and the distribution of stress in goaf is not uniform, resulting in the distribution of particle size and compaction degree of mined-out coal. It is necessary to carry out experimental studies on coal crushing granularity and compaction degree under different loads and loading processes to clarify its distribution law. Therefore, experiments on the coal crushing were conducted, to analyze the compression behaviors and the distributions of the particle size with different loading speeds and loads. The results show that, in the process of slow pressure application, the lump coal was constantly compressed, compacted, and broken. With the increase in the axial load, the coal compressibility increased, and the coefficient of fragmentation and porosity decreased. When the stress was greater than the compressive strength, the variation trend slowed. When the stress was greater than two times the strength, as the load continued to increase, compression basically did not occur. The thickness and porosity of coal will be reduced to 0.5 times that of loose coal when a significant change of the compression ratio occurs. After the coal body was under pressure, the degree of crushing intensified. The fractal dimension of the particle sizes of broken coal particles followed a logarithmic relationship with the increase in the stress. With the increase of stress, the degree of crushing increased, and in the process of pressure crushing, the particle size of 2.5 mm was an important boundary. When the stress was more than two times the strength value, the degree of crushing under the increased load did not increase significantly. When the residual coal in a goaf is affected by pressure, if there is no impact, the influence of the initial pressure and periodic pressure variations on the residual coal in the goaf will not be significant, and the accumulation and crushing degree of residual coal will only be affected by the peak stress.

## 1. Introduction

There are many types of disasters in coal mine goafs. The disaster-causing factors are complex and coupled, and they show dynamic changes as the working surfaces are advanced [1]. During the mining of a coal mining face, the residual coal in the goaf experiences three stages: the natural expansion zone, the stress recovery zone, and the original rock stress zone [2]. The stress recovery in a mined-out area is related to the buried depth and mining procedure, and the depth and process determine the magnitude of the stress [3, 4]. The stress loading has a significant effect on the expansion coefficient and porosity of broken coal [5–7]. The

fragmentation coefficient has an influence on the flow pattern, O<sub>2</sub> volume fraction distribution, and temperature distribution. Owing to the stress recovery in the goaf, the coefficient of fragmentation and expansion of broken coal varies, which leads to changes in the porosity and permeability. This has an important impact on the occurrence of coal spontaneous combustion. The process of spontaneous combustion is primarily influenced by the temperature, oxidation history of coal, coal properties, particle size distribution of the coal, coal thickness, air leakage, and porosity. A change of the structure will significantly change the spontaneous combustion characteristics of coal [8]. Yang et al. [9] pointed out that, with the increase in the axial

pressure on coal samples, the fractal dimension of the particles increased, and the specific surface area increased, which was conducive to the formation of free radicals. This led to an increase in the apparent thermal conductivity, accelerating the process of coal-oxygen composite oxidation and promoting the improvement of the coal temperature and the acceleration of the reaction process. Ma et al. [10–12] study showed that, under the influence of water and pressure or stress, gangue generally showed a decrease in strength, an increase in crushing ratio, and a decrease in porosity and permeability.

The crushing of raw coal consumes a huge amount of energy, and generally, the coal strength must be overcome. When the load is large and the coal is fully compacted, it will enter a compaction crushing state [13–16]. The crushing of coal is affected by its strength, local particle size, and impact energy [17–21]. The coal loading process leads to compression and fragmentation, which are key influencing factors of residual coal spontaneous combustion in goafs.

The oxidation tests of coal samples by Küçük et al. [22] showed that the particle size is an important factor affecting coal spontaneous combustion. The smaller the particle size is, the greater the tendency for coal spontaneous combustion becomes. Wang et al. [23] proved that the spontaneous combustion tendency of lignite increases with a decrease in the particle size. The essence of coal spontaneous combustion is that some active structures on the coal surface contact oxygen in the air, resulting in coal-oxygen complex reactions [24–29]. Coal contains many functional groups. Among them, oxygen-containing functional groups such as carboxyl and carbonyl groups can be thermally decomposed to generate free radical active sites, which have an oxidation effect and accelerate the spontaneous combustion [30–33]. The large amount of mechanical energy applied to coal during crushing not only refines the appearance of the grains of coal particles and increases the specific surface area but also oxidizes coal through the chemical action caused by the mechanical forces [34, 35].

The significant influence of the particle size on the coal spontaneous combustion of residual coal in a goaf was examined in this study. From a macroperspective, it is crucial to first determine the crushing state of residual coal under the pressure distribution in the goaf. Only by determining the crushing state, particle size composition, compaction and expansion parameters, porosity, and permeability of coal under different pressure distributions in the goaf can the variations of the spontaneous combustion process of residual coal in the goaf under different external and internal factors be further studied, which would allow the spontaneous combustion process and distribution of residual coal in the goaf to be described and predicted more accurately. Therefore, the compression, compaction, and crushing experiments of lump coal under different axial pressures were conducted to study the compression, swelling, and particle size distribution after the crushing of coal under different pressures.

## 2. Experimental Methods

**2.1. Strength Test and Calculation Method Based on Point-Load.** According to the GB/T50266-1999 standard, a point-loading experiment was conducted using the multifunctional digital display 100-kN rock point-load tester (HDS-1) produced by Shandong Jinan Mining and Rock Test Instrument Co., Ltd. The load limit and displacement were analyzed to determine the compressive and tensile strengths of lignite.

The uncorrected point-load strength index is defined as follows:

$$I_s = \frac{P}{D_e^2}, \quad (1)$$

where  $I_s$  is the uncorrected point-load strength index (MPa),  $P$  is the failure load (N), and  $D_e$  is the equivalent core diameter (mm).

For square or irregular coal and rock blocks, the equivalent core diameter basis  $D_e$  is calculated as follows:

$$D_e = \frac{4WD'}{\pi}, \quad (2)$$

where  $W$  is the width (or mean width) of the minimum cross section through two loading points (mm), and  $D'$  is the spacing of the loading points (mm).

The modified point-load intensity index ( $I_{s50}$ ) is defined as follows:

$$I_{s50} = FI_s, \quad (3)$$

where  $I_{s50}$  is the modified point-load strength index (MPa), and  $F$  is a geometric correction factor, calculated as follows:

$$F = \left(\frac{D_e}{50}\right)^{0.45}, \quad (4)$$

where  $D_e$  is the equivalent core diameter (mm).

**2.2. Experimental Method and Process of Crushing under Pressure.** A round-hole standard sieve was used to screen the coal samples after simple manual crushing. Coal samples with particle sizes of 20–30 mm were selected and loaded into a crushing tank, and the height of the coal sample in the tank is 100 mm. The crushing tank was placed on the universal press to conduct the crushing experiments. During the crushing experiment, 5 maximum loads were set, and each maximum load corresponded to 3 different loading speeds. There were 15 coal samples in total. The canning mass of coal samples was shown in Table 1, and the initial canning height was all 100 mm. The loading speed and maximum load are set on the press. During the experiment, the quasistatic load application speed of the press was set to 0.5, 1 and 2 kN/s, and the maximum quasistatic load was set to 50, 100, 200, 300, or 400 kN. After reaching the corresponding

TABLE 1: Canning quality of coal samples under different loading experimental conditions.

$V_{sl}$ (kN/s)	F (kN)				
	50 (g)	100 (g)	200 (g)	300 (g)	400 (g)
0.5	1194	1200	1205	1195	1178
1.0	1217	1234	1145	1184	1170
2.0	1229	1210	1188	1182	1231

maximum quasistatic load, the load was held for 5 s and then unloaded. To ensure the consistency of particle size of coal samples before crushing, the coal samples for each crushing experiment should be used only once and not reused. After that, the coal sample is taken out for screening and weighing, and then the sample is sealed and stored for use in other experiments. Then the particle size distribution of lignite after crushing under different crushing conditions was analyzed.

### 3. Analysis and Discussion of Experimental Results

**3.1. Compressive Strength Analysis of Lignite.** The experiments were conducted using a 100 kN point-load press produced by Shandong Institute of Mining and Rock, and a newly cut coal block at the working face was selected as the sample. After the sample was selected, point loading was conducted in the vertical bedding direction. Before loading, the average width  $W$  of the surface between the loading points was measured, and the spacing  $D$  of the loading points was recorded. In the loading process, the displacement  $L$  and the maximum loading force  $F$  were recorded. The displacement was the penetration depth between the two points. When calculating the point-load strength,  $D$  minus the penetration depth of the loading point was the real loading distance  $D'$ . Based on this, the uncorrected point-load intensity index  $I_s$  was calculated by equations (1) and (2), and then the corrected point-load intensity index  $I_{s50}$  was calculated using equations (3) and (4). The relevant data and calculation results of the point-loading experiment are shown in Table 1.

A total of 35 samples were selected in the process of the point-loading test, and fracture occurred in 27 of the experiments. The relevant effective experimental results are shown in Table 1. After the normal distribution detection, the maximum loading force or breaking force of 27 groups of effective experimental data obtained from the experiment followed a normal distribution, and these data could be used for calculation and analysis.

Table 1 shows that the maximum point-load strength index  $I_{s50}$  of the 27 groups of effective experiments was 0.49 MPa, and the minimum point-load strength index was 0.11 MPa. According to the point-load experimental processing method, for more than 21 groups of effective loading data, the maximum and minimum values of the first and last two groups were removed, and the average value of the other numerical calculations was retained as the mean value of the point-load strength index. The  $I_{s50}$  value of lignite was 0.32 MPa.

TABLE 2: Relevant parameters of point-load test and calculation results of strength index.

Numbered	W (mm)	D (mm)	P (kN)	$I_s$ (MPa)	F/1	$I_{s50}$ (MPa)
1	85	60	1.49	0.25	1.22	0.30
2	96	54	1.86	0.31	1.22	0.38
3	104	90	2.06	0.18	1.41	0.25
4	82	75	1.88	0.26	1.27	0.33
5	83	71	1.56	0.22	1.26	0.28
6	117	95	2.09	0.16	1.46	0.23
7	96	55	2.04	0.33	1.23	0.40
8	98	50	1.38	0.24	1.21	0.29
9	102	82	3.51	0.36	1.36	0.49
10	65	55	0.44	0.10	1.13	0.11
11	74	52	0.92	0.20	1.14	0.23
12	140	55	1.77	0.20	1.33	0.26
13	81	62	0.94	0.16	1.22	0.19
14	83	65	1.49	0.23	1.24	0.28
15	104	55	1.28	0.19	1.25	0.24
16	109	57	1.42	0.19	1.28	0.24
17	132	65	2.64	0.27	1.36	0.37
18	75	60	1.56	0.29	1.19	0.35
19	109	52	1.62	0.24	1.25	0.30
20	109	65	2.85	0.36	1.30	0.46
21	113	56	1.84	0.24	1.28	0.31
22	108	66	2.49	0.30	1.31	0.39
23	67	50	1.29	0.32	1.11	0.36
24	83	55	1.67	0.34	1.16	0.40
25	73	55	1.52	0.32	1.15	0.37
26	75	70	2.2	0.37	1.22	0.45
27	68	55	1.57	0.36	1.13	0.41

Average value  $I_{s50} = 0.32$  MPa after removing the minimum and maximum data.

The conversion relationship between the load strength and the compressive strength of the coal system rock points given in 2014 by Kahraman [36] is as follows:

$$Re = 23.62I_{s50} - 2.69. \quad (5)$$

Based on the uniaxial compressive strength  $Re = 4.87$  MPa,  $I_{s50} = 0.11$  MPa.

The conversion method proposed by Kassim [37] in 2007 is as follows:

$$\begin{cases} I_s < 1\text{MPa}, & Re = 12.23I_{s50} + 1.75, \\ I_s > 1\text{MPa}, & Re = 14.45I_{s50} + 0.096, \\ I_s < 2\text{MPa}, & Re = 13I_{s50}, \\ I_s = 2 - 5\text{MPa}, & Re = 24I_{s50}, \\ I_s > 5\text{MPa}, & Re = 28I_{s50}. \end{cases} \quad (6)$$

As shown in Table 2, for 27 groups of effective experiments,  $I_s$  was less than 1 MPa, and it was determined that  $Re = 5.66$  MPa. Therefore, the uniaxial compressive strength  $Re$  of the coal was 4.87–5.66 MPa.

The conversion relationship between the point-load and uniaxial tensile strength is like that between the point-load and the uniaxial compressive strength. Various scholars have presented different methods:

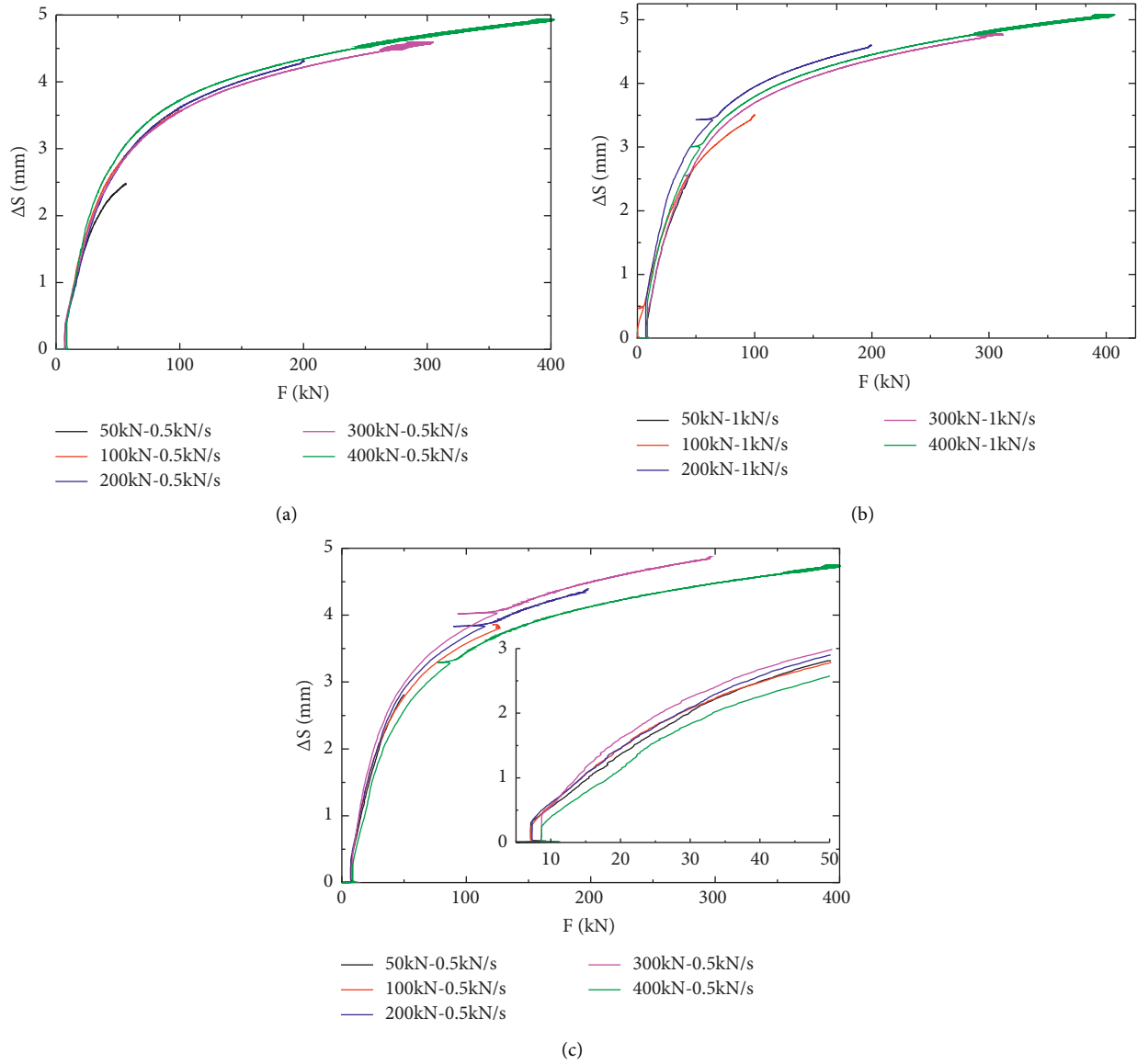


FIGURE 1: Variations of displacement with time and quasistatic load under loading speeds of 0.5–2.0 kN/s. (a) Loading speed 0.5 kN/s. (b) Loading speed 1.0 kN/s. (c) Loading speed 2.0 kN/s.

$$\begin{cases} R_t = 2.92I_{s50}^{[38]}, \\ R_t = 1.25I_{s50}^{[39]}, \\ R_t = 1.50I_{s50}^{[40]}, \\ R_t = 0.96I_{s50}^{[41]}, \end{cases} \quad (7)$$

where  $R_t$  is the uniaxial tensile strength, MPa.

According to the research suggestions of Li et al. [42], the formula established by Wang et al. [38] is of high reliability to calculate the tensile strength, so we also use this method to calculate it; the uniaxial tensile strength ( $R_t$ ) is about  $2.92 \times 0.32 = 0.93$  MPa.

**3.2. Compression and Expansion Analysis of Crushing Process under Pressure.** The variations of the displacement ( $\Delta S$ ,

mm/10 mm) with the time ( $t$ , s) and load ( $F$ , kN) in the crushing process of lignite under conditions with quasistatic load velocities ( $V_{sb}$ , kN/s) of 0.5, 1.0, and 2.0 kN/s are shown in Figure 1. Under the same quasistatic load velocity, the larger the maximum load was, the larger the displacement was, which indicated that the larger the quasistatic load was, the higher the compression degree of lump lignite was. The relationships between the compression amounts of the coal samples and the load were different for the three different loading speeds. When the maximum loads were 50 and 100 kN, the compression amount increased rapidly with the increase in the load, basically following a linear relationship. When the load was greater than 100 kN, the compression amount increased slowly with the increase in the load. When the axial stress of the coal sample was not greater than its strength, the compression amount increased significantly and rapidly with the increase in the stress. When the stress

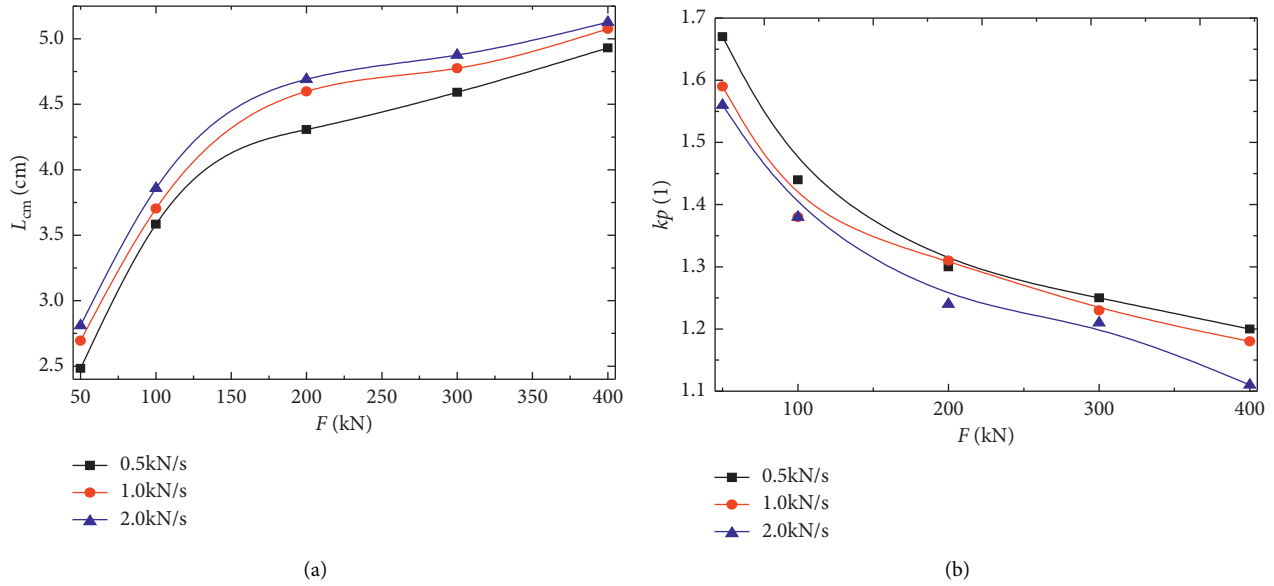


FIGURE 2: Variations of compression and swelling coefficient of 100 mm coal sample with the maximum quasistatic load and stress under different quasistatic load application speeds. (a) Change of compression volume. (b) Change of fragmentation and expansion coefficient.

was greater than its strength, the stress increased continuously, and the compression amount no longer increased significantly. When the stress reached twice the strength, the stress increased continuously, and the compression amount basically no longer increased.

The variations of the compression (amount of compression,  $L_{AM}$ , cm) of the 100 mm high coal sample with the quasistatic load and the corresponding stress ( $E$ , MPa) calculated under different quasistatic load velocities and maximum loads are shown in Figure 2. The results show that the compression increased significantly with the increase in the quasistatic load velocity and quasistatic load or stress. At the same time, based on the variations of the compression dilatancy coefficient of the coal samples under different maximum loads in the figure, with the increase in the load, the compression dilatancy coefficient decreased. When the load application speed was small, the corresponding compression amount was small, and the dilatancy coefficient was large. The correlation test was conducted using the SPSS software. The test results showed that the maximum load was negatively correlated with the swelling coefficient at the 0.01 level, and the correlation coefficient was  $-0.904$ . There was no significant correlation between the loading speed and the swelling coefficient and porosity.

After crushing the lignite under pressure, there was a logarithmic relationship between the height decrease and stress of the 100 mm high lignite after compaction; that is, with the increase in the load, the compression amount increased, and the coefficient of fragmentation decreased. However, when the load was large, as the load was increased continuously, the increase in the compression amount and the decrease in the coefficient of fragmentation slowed, and no significant change was observed. This indicated that the compression and fragmentation of lignite will no longer occur when the load increases to a certain extent.

Under different vertical stress conditions, the compaction compression amounts of naturally accumulated lignite were quite different. When the loads were 50, 100, 200, 300, and 400 kN (vertical stresses of 2.76, 5.51, 11.03, 16.54, and 22.06 MPa), and the loading speeds were 0.5, 1, and 2, the average compression ratios were 17%, 27%, 35%, 37%, and 40%, respectively. This indicated that when the axial stress generated by the vertical load was about twice the compressive strength or more, the compression amount of coal no longer significantly increased, and the coefficient of fragmentation and expansion no longer significantly decreased. The relationship can be expressed as follows:

$$kp(E) = 1.8417E^{-0.148} (R^2 = 0.9872). \quad (8)$$

With the increase in the load or stress, the expansion coefficient decreased exponentially. When the stress was large, the expansion coefficient no longer decreased significantly.

Figure 3 shows the average expansion coefficient and mean porosity curves of the compressed coal under different maximum load conditions. At loads of 50, 100, 200, 300, and 400 kN (corresponding to vertical stresses of 2.76, 5.51, 11.03, 16.54, and 22.06 MPa, respectively), the average expansion coefficients were 1.61, 1.40, 1.28, 1.23, 1.16, respectively, and the corresponding mean porosities were 0.38, 0.29, 0.22, 0.19, and 0.14. That is, the expansion coefficient and porosity of the compressed coal decreased.

**3.3. Crushed Particle Size Analysis.** The mass percentage distribution of particle size under different loading conditions is shown in Figure 4. The results showed that, in the crushed coal, a large particle size accounted for a large proportion of the particles, and the smaller the particle size

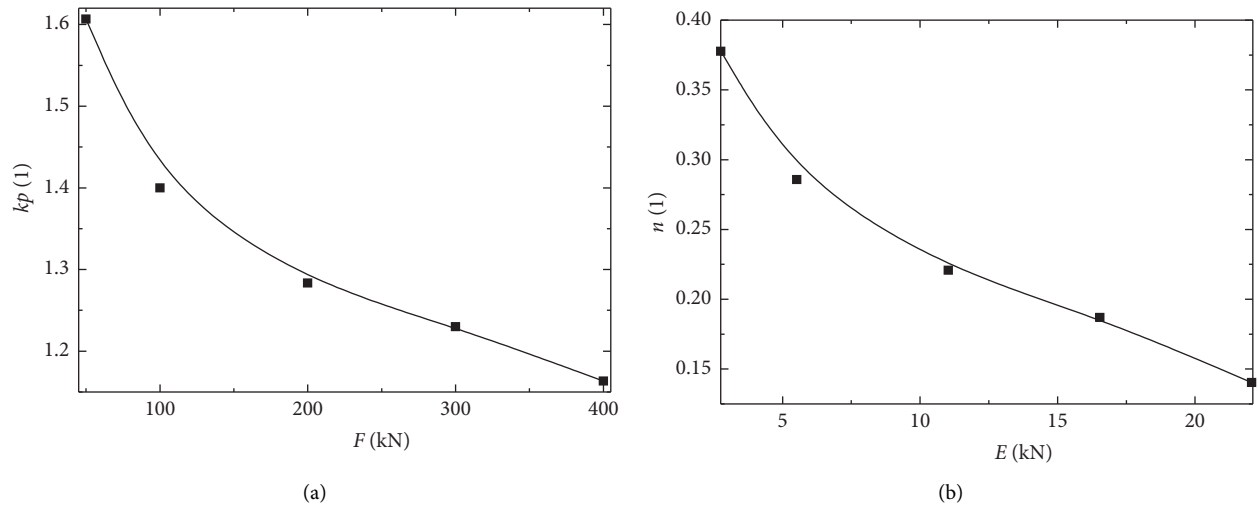


FIGURE 3: Variations of crushing expansion coefficient and porosity with load. (a) Crushed compaction expansion coefficient with load. (b) Variation of porosity with stress.

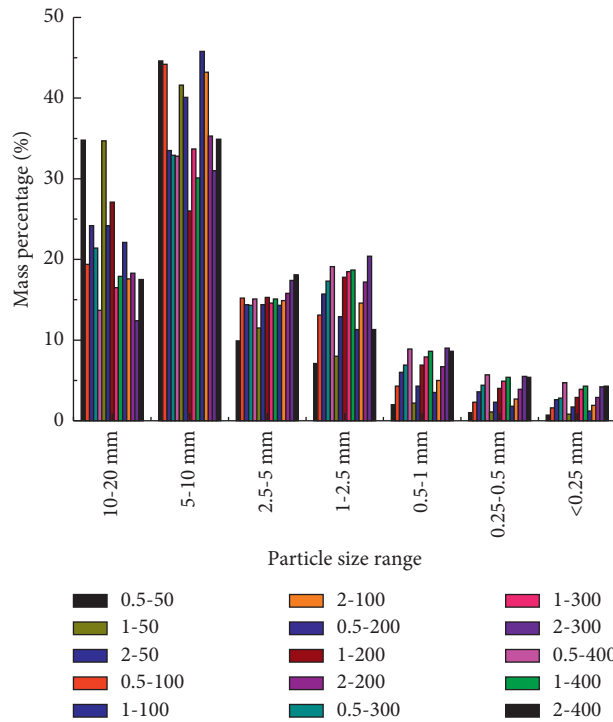


FIGURE 4: Mass percentage distribution of particle size under different loading conditions.

was, the lower the proportion was. The mass ratios of the coal samples with particle sizes greater than 2.5 mm in broken coal decreased with the increase in the load, and the mass ratio of the coal samples with particle sizes less than 2.5 mm increased with the increase in the load.

Based on the theory of the fractal dimension ( $D$ ) of the particle size, Xie [43] defined the particle size distribution function as follows:

$$Y_n(x) = \frac{(N_t - N)}{N_t}, \quad (9)$$

where  $x$  is the particle of coal sample,  $N_t$  is the total number of particles,  $N$  is the total number of particles larger than size  $x$ , and  $N_t - N$  is the number of particles smaller than size  $x$ .

The number of particles  $dN$  in the system between sizes  $x$  and  $x + dx$  is as follows:

$$dN = N_t dY_n(x). \quad (10)$$

From equation (9), the following can be obtained:

$$Y_n(x) = \frac{(N_t - N)}{N_t \%} = \left( \frac{1 - N}{N_t} \right) \%. \quad (11)$$

The particle size distribution can be expressed as a fractal, as follows:

$$Y_n(x) \sim -x^{-D}. \quad (12)$$

The particle size from the compression and crushing process of granular particles follows fractal distributions in nature. The number of characteristic scales of the particle size distribution based on equation (12) is as follows:

$$N(x > d) = Cd^{-D}, \quad (13)$$

where  $d$  is the coal sample characteristic scale,  $n$  is the number of coal particles whose diameters are larger than the characteristic scale,  $C$  is a constant, and  $D$  is the Hausdorff fractal dimension of the particle size distribution.

The quality of the coal samples and particle diameter satisfy the following relationship:

$$M_d(x < d) = \int_{d_{\min}}^d spx^3 N(x), \quad (14)$$

where  $s$  represents the shape coefficient, and  $d_{\min}$  represents the minimum particle size in the sample.

Combining equations (13) and (14) yields the following:

$$M_d(x < d) = \frac{CDs\rho}{3-D} (d^{3-D} - d_{\min}^{3-D}),$$

$$M_t = M_d(x < d_{\min}) = \frac{CDs\rho}{3-D} (d_{\min}^{3-D} - d_{\min}^{3-D}),$$

$$\frac{M_d(x < d)}{M_t} = \left( \frac{d}{d_{\max}} \right)^{3-D},$$

$$(3-D) \lg \left( \frac{d}{d_{\max}} \right) = \lg \left( \frac{M_d(x < d)}{M_t} \right), \quad (15)$$

where  $C$  is the proportional constant,  $\rho$  is the particle mass density,  $M_d$  is the mass of particles with particle size less than  $d$ ,  $M_t$  is the total mass of coal sample, and  $d_{\max}$  is the maximum particle size of coal sample particles.  $d_{\min}$  is the minimum particle size of coal sample particles which is 0; with  $\lg(d/d_{\max})$  as the abscissa and  $\lg(M_d(x < d)/M_t)$  as the ordinate, the slope of the fitted straight line is  $3D$ .

The fractal dimensions of the particle size under different maximum loads and loading speeds are shown in Table 3. An SPSS correlation test showed that there was a significant positive correlation between the fractal dimension and maximum load at the 0.01 level, and the correlation coefficient was 0.938. There was no significant correlation between the fractal dimension and load application speed.

The logarithmic relationship between the average fractal dimension of the particle size and the load at three loading speeds under the same maximum load is shown in Figure 5, and it is expressed as follows:

$$D = 0.18 \ln(E) + 1.68, \quad (16)$$

$$R^2 = 0.9958.$$

TABLE 3: Fractal dimensions of particle size under different maximum loads and loading speeds.

E (kN)	V <sub>sl</sub> (kN/s)			Average
	0.5	1	2	
2.76	1.81	1.83	1.90	1.85
5.51	1.96	1.99	2.00	1.99
11.03	2.11	2.14	2.11	2.12
16.54	2.12	2.19	2.19	2.17
22.06	2.23	2.22	2.24	2.23

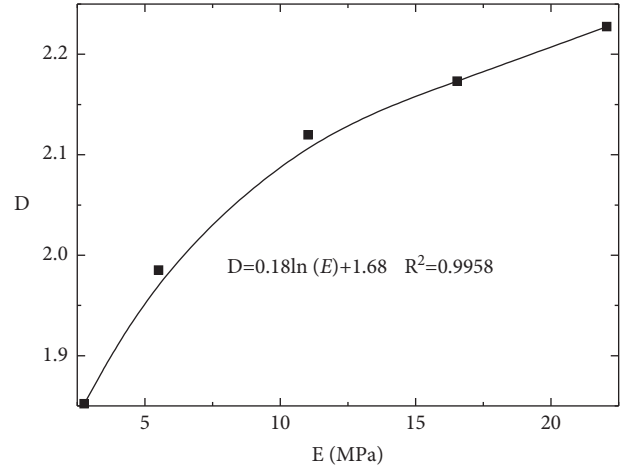


FIGURE 5: Variation of fractal dimension of particle size with maximum stress.

That is, there was a nonlinear relationship between the fractal dimension of the particle size of the crushed coal and the stress. When the stress was less than two times the compressive strength, the stress increased, the fractal dimension of the particle size increased, and the proportion of continuous crushing of the coal increased. When the stress was greater than twice the compressive strength of the coal, the stress continued to increase, and the degree of coal crushing no longer significantly increased, which is basically consistent with the conclusions of Zhang et al. [14].

#### 4. Discussion

In the experiments, with the increase in the axial load of lignite, the volume of lignite decreased, and the shrinkage rate increased linearly and rapidly with the increase in the load. When the axial stress was greater than the strength of the coal, upon increasing the load, the compression rate of the coal increased slowly. When the stress was greater than two times the strength, when increasing the load continuously, the coal was no longer compressed. The coal compression process was accompanied by a decrease in the swelling coefficient, porosity, and particle breakage. During the crushing process of the coal samples used in the experiments, with the increase in the load, a particle size of 2.5 mm was taken as the boundary. The proportion of

broken particles larger than 2.5 mm decreased gradually, and the proportion of broken particles smaller than 2.5 mm increased gradually. The fractal dimension of the particle size can be used to describe the degree of particle breakage. With the increase in the load and stress, the fractal dimension of the particle size increased, and the degree of particle breakage increased. There was a logarithmic relationship between the fractal dimension of the particle size and the axial stress. However, when the axial stress was greater than two times the strength, the fractal dimension no longer significantly increased, and the particles were no longer broken.

During the normal mining of a working face, the scope of the goaf expands with the advancing of the working face. The strata in the mined-out area will collapse orderly, and the pressure of the residual coal caving in the mined-out area will also change dynamically, including the initial pressure and the periodic pressure. The above dynamic changes determine that the thickness, porosity, and crushing degree of the coal rock at any point in the goaf change dynamically before entering the deep part of the goaf or until the stress reaches twice the strength. The air leakage intensity, oxygen supply, and heat accumulation and loss in the goaf will change dynamically, and various factors will jointly lead to dynamic changes of the spontaneous combustion process of the residual coal in the goaf. If a dynamic change of the working face with a large dip angle occurs, the stress distribution in the goaf will possess asymmetric spatial characteristics, especially in the middle and lower parts of the working face, the stress will be relatively concentrated, and the variation range will be large. The thickness, porosity, air leakage flow, and oxygen supply capacity of the residual coal will show more significant changes. It is necessary to consider the dynamic asymmetric changes of the stress to accurately describe and determine the spontaneous combustion characteristics of residual coal. Therefore, to study the spontaneous combustion of residual coal in a goaf, we must pay attention to and correctly describe these dynamic changes in the goaf.

Coal mine goaf with working face advancing is a dynamic area; therefore, the release of the deformation and force of roof and floor of mined-out area is dynamic changes, combined with the stress distribution of goaf form; on different positions and at different times in the mined-out area, the stress distribution of the mined-out area is different, unless deeper in the gob area stress is basically stable. And all kinds of disasters in mined-out area mainly occur in the dynamic area, such as heritage coal mined-out area affected by the incoming wind leakage occurring in the course of spontaneous combustion, etc., according to common sense, and the results of the study have been publicly reported, and the compaction state of coal goaf air leakage and oxygen supply and crushing grain size directly affect the heat transfer, in order to accurate the traces of goaf coal spontaneous combustion oxidation process and location forecast. Therefore, the research results of this paper can provide theoretical support for prediction and prevention and control of problems such as spontaneous combustion of abandoned coal in goaf and emission of toxic and harmful gases.

## 5. Conclusions

- (1) For the loose coal under pressure, as the axial load of the coal increased, the compression rate of the coal increased, the swelling coefficient decreased, and the porosity decreased. When the stress was greater than the compressive strength, there was no evident linear increase. When the stress was more than twice the strength, as the load continued to increase, compression basically did not occur.
- (2) The degree of crushing was increased after the coal was under pressure. The fractal dimension of the broken coal particle size followed a logarithmic relationship with the increase in the stress. The stress increased, and the degree of crushing increased. The particle size of 2.5 mm was an important boundary in the process of crushing under pressure. With the increase in the stress, the proportion of broken coal larger than 2.5 mm decreased, and the proportion of broken coal smaller than 2.5 mm increased. When the stress was more than twice the strength, the load crushing degree no longer increased significantly.
- (3) When the loading speed was less than 2 kN/s, the compression, expansion coefficient, porosity, and fractal dimension of the particle size of the coal body were significantly correlated with the stress and were not significantly affected by the loading speed, and the accumulation state and crushing degree of residual coal are only affected by the peak stress.

## Data Availability

The data used to support the findings of this study are included within the article.

## Conflicts of Interest

The authors declare that they have no conflicts of interest or personal relationships that could have appeared to influence the work reported in this paper.

## Acknowledgments

The authors thank LetPub ([www.letpub.com](http://www.letpub.com)) for its linguistic assistance during the preparation of this article. This research was supported by the National Natural Science Foundation of China (Grant no. 51804107), Natural Science Foundation of Hunan Province (Grant nos. 2020JJ4260 and 2019JJ50109), and the Key Projects of Hunan Education Department (Grant nos. 20A142, 19A123, 19B138, and 18A420).

## References

- [1] B. Q. Lin, Q. Z. Li, and Y. Zhou, "Research advances about multi-field evolution of coupled thermodynamic disasters in coal mine goaf," *Journal of China Coal Society*, vol. 46, no. 6, pp. 1715–1726, 2021.
- [2] M. G. Qian and J. L. Xu, "Study on the "O-shapecircle" distribution characteristics of mining-induced fractures in the

- overlying strata,” *Journal of China Coal Society*, vol. 23, no. 5, pp. 466–469, 1998.
- [3] J. Conroy, “Influence of elevated atmospheric CO<sub>2</sub> concentrations on plant nutrition,” *Australian Journal of Botany*, vol. 40, no. 5, pp. 445–456, 1992.
- [4] H. Yavuz, “An estimation method for cover pressure re-establishment distance and pressure distribution in the goaf of longwall coal mines,” *International Journal of Rock Mechanics and Mining Sciences*, vol. 41, no. 2, pp. 193–205, 2004.
- [5] L. M. Xu, Y. S. Pan, Z. H. Li, A. W. Wang, and L. Geng, “Similarity simulation experiment of deformation of deep mining-induced overburden stress,” *Chinese Journal of Geological Hazard and Control*, vol. 22, no. 3, pp. 61–66, 2011.
- [6] X. X. Miao, X. B. Mao, G. W. Hu, and Z. G. Ma, “Research on broken expand and press solid characteristics of rocks and coals,” *Journal of Experimental Mechanics*, vol. 12, no. 3, pp. 394–400, 1997.
- [7] S. G. Li and M. G. Qian, “Features of fallen rock and methane flow characteristics in gob of fully-mechanized working-face with top-coal caving ground,” *Pressure and Strata Control*, vol. 3, no. 4, pp. 76–78, 1997.
- [8] T. X. Chu, X. F. Han, and M. G. Yu, “Low-temperature oxidation characteristics of compacted broken coal and macroscopic cause analysis,” *China Safety Science Journal*, vol. 29, no. 9, pp. 77–83, 2019.
- [9] Y. M. Yang, J. Z. Liu, X. He, Z. H. Wang, J. H. Zhou, and K. F. Cen, “Research status of drying and crushing characteristics of lignite,” *Thermal power ceneratton*, vol. 46, no. 5, pp. 14–20, 2017.
- [10] D. Ma, S. Kong, Z. Li, Q. Zhang, Z. Wang, and Z. Zhou, “Effect of wetting-drying cycle on hydraulic and mechanical properties of cemented paste backfill of the recycled solid wastes,” *Chemosphere*, vol. 282, Article ID 131163, 2021.
- [11] D. Ma, J. Zhang, H. Duan et al., “Reutilization of gangue wastes in underground backfilling mining: overburden aquifer protection,” *Chemosphere*, vol. 264, Article ID 128400, 2021.
- [12] D. Ma, H. Duan, J. Liu, X. Li, Z. L. Zhou, and Z. Zhou, “The role of gangue on the mitigation of mining-induced hazards and environmental pollution: an experimental investigation,” *The Science of the Total Environment*, vol. 664, no. 1, pp. 436–448, 2019.
- [13] J. W. Chen, *Study on Seepage Characteristics and Particle Size Distribution of Mixed Broken Coal Samples*, Xi’an University of Science and Technology, Xian, China, 2019.
- [14] T. J. Zhang, J. W. Chen, R. Y. Bao, X. K. Jiang, A. Zhou, and D. Ge, “Fractal characteristics of particle size distribution of broken coal samples with different immersion time,” *Journal of Mining & Safety Engineering*, vol. 35, no. 3, pp. 598–604, 2018.
- [15] C. Zhang, Y. X. Zhao, S. H. Tu et al., “Influence mechanism of particle size on compaction and crushing characteristics of broken coal in goaf,” *Journal of Coal*, vol. 22, no. 2, pp. 69–74, 2020.
- [16] J. S. Esterle, Y. Kolatschek, and G. O’Brien, “Relationship between in situ coal stratigraphy and particle size and composition after breakage in bituminous coals,” *International Journal of Coal Geology*, vol. 49, no. 2-3, pp. 195–214, 2002.
- [17] M. Onifade and B. Genc, “A review of research on spontaneous combustion of coal,” *International Journal of Mining Science and Technology*, vol. 30, no. 3, pp. 303–311, 2020.
- [18] E. M. Suuberg, Y. Otake, Y. Yun, and S. C. Deevi, “Role of moisture in coal structure and the effects of drying upon the accessibility of coal structure,” *Energy & Fuels*, vol. 7, no. 3, pp. 384–392, 1993.
- [19] R. Fry, S. Day, and R. Sakurovs, “Moisture-induced swelling of coal,” *International Journal of Coal Preparation and Utilization*, vol. 29, no. 6, pp. 298–316, 2009.
- [20] S. R. Kelemen, L. M. Kwiatek, M. Siskin, and A. G. K. Lee, “Structural response of coal to drying and pentane sorption,” *Energy & Fuels*, vol. 20, no. 1, pp. 205–213, 2006.
- [21] Y. Qin, H. Song, and W. Liu, “Experimental study on impact of dispersion of coal particles for residual coal spontaneous combustion,” *Safety In Coal Mines*, vol. 46, no. 1, pp. 22–25, 2015.
- [22] A. Küçük, Y. Kadioğlu, and M. S. Gülaboğlu, “A study of spontaneous combustion characteristics of a Turkish lignite: particle size, moisture of coal, humidity of air,” *Combustion and Flame*, vol. 133, no. 3, pp. 255–261, 2003.
- [23] D. Wang, G. Dou, X. Zhong, H. Xin, and B. Qin, “An experimental approach to selecting chemical inhibitors to retard the spontaneous combustion of coal,” *Fuel*, vol. 117, pp. 218–223, 2014.
- [24] B. Qin, G. Dou, Y. Wang, H. Xin, L. Ma, and D. Wang, “A superabsorbent hydrogel-ascorbic acid composite inhibitor for the suppression of coal oxidation,” *Fuel*, vol. 190, pp. 129–135, 2017.
- [25] J. Deng, C. K. Lei, K. Cao, L. Ma, Y. Xiao, and L. Ren, “Support vector regression approach for predicting coal spontaneous combustion,” *Journal of Xi’an University of Science and Technology*, vol. 38, no. 2, pp. 175–180, 2018.
- [26] K. Wang, X. Zhai, W. Wang, and H. Wen, “Effect of oxygen concentration and blowing rate on thermal properties of coal,” *Journal of Xi’an University of Science and Technology*, vol. 38, no. 01, pp. 31–36, 2018.
- [27] W. Cheng, X. Hu, J. Xie, and Y. Zhao, “An intelligent gel designed to control the spontaneous combustion of coal: fire prevention and extinguishing properties,” *Fuel*, vol. 210, pp. 826–835, 2017.
- [28] Y. Liang, J. Zhang, T. Ren, Z. Wang, and S. Song, “Application of ventilation simulation to spontaneous combustion control in underground coal mine: a case study from bulianta colliery,” *International Journal of Mining Science and Technology*, vol. 28, no. 2, pp. 231–242, 2018.
- [29] H. Wang, B. Z. Dlugogorski, and E. M. Kennedy, “Thermal decomposition of solid oxygenated complexes formed by coal oxidation at low temperatures,” *Fuel*, vol. 81, no. 15, pp. 1913–1923, 2002.
- [30] H. Wang, B. Z. Dlugogorski, and E. M. Kennedy, “Coal oxidation at low temperatures: oxygen consumption, oxidation products, reaction mechanism and kinetic modelling,” *Progress in Energy and Combustion Science*, vol. 29, no. 6, pp. 487–513, 2003.
- [31] C. Zhou, Y. Zhang, J. Wang, S. Xue, J. Wu, and L. Chang, “Study on the relationship between microscopic functional group and coal mass changes during low-temperature oxidation of coal,” *International Journal of Coal Geology*, vol. 171, pp. 212–222, 2017.
- [32] Y. Zhang, J. Wang, S. Xue et al., “Evaluation of the susceptibility of coal to spontaneous combustion by a TG profile subtraction method,” *Korean Journal of Chemical Engineering*, vol. 33, no. 3, pp. 862–872, 2016.
- [33] Q. Hou, Y. Han, J. Wang, Y. Dong, and J. Pan, “The impacts of stress on the chemical structure of coals: a mini-review based on the recent development of mechanochemistry,” *Science Bulletin*, vol. 62, no. 13, pp. 965–970, 2017.

- [34] J. Li, Z. Li, Y. Yang, C. Wang, and L. Sun, "Experimental study on the effect of mechanochemistry on coal spontaneous combustion," *Powder Technology*, vol. 339, pp. 102–110, 2018.
- [35] Z. Dong, L. Sun, T. Jia et al., "Rapid contrastive experimental study on the adiabatic spontaneous combustion period of loose lignite," *ACS Omega*, vol. 6, no. 50, pp. 34989–35001, 2021.
- [36] S. Kahraman, "The determination of uniaxial compressive strength from point load strength for pyroclastic rocks," *Engineering Geology*, vol. 170, pp. 33–42, 2014.
- [37] A. Kassim, *Mohammad. Laboratory Study of Weathered Rock for Surface Excavation Works*, Universiti Teknologi Malaysia, Johor Bahru, Malaysia, 2007.
- [38] W. G. Wang and M. L. Wang, "Errors and correlation analysis of point load tests," *Rock mechanics and engineering*, vol. 7, no. 4, p. 310, 1988.
- [39] R. Wang, C. A. Tang, and S. H. Wang, "Study on several problems about point load test of rock," *Journal of North-eastern University*, vol. 29, no. 1, pp. 130–140, 2008.
- [40] F. Yang and Y. L. Xie, "Determination of the rock strength with point load test," *Journal of Guangxi University (Natural Science Edition)*, vol. 38, no. 1, pp. 138–143, 2013.
- [41] China Communications Group No.2 Highway Survey and Design Institute, *Highway Engineering Rock Test procedures: JTGE41-2005*, People's Transportation Press, Beijing, 2005.
- [42] H. P. Li, Y. Y. Wu, C. Ge, L. Dai, and H. Y. Yao, "Study on the relation between point load strength and compressive and tensile strength of marble," *Science Technology and Engineering*, vol. 19, no. 32, pp. 294–299, 2019.
- [43] H. P. Xie, "Fractal pores and fractal particles of rock and soil materials," *Advances in Mechanics*, vol. 23, no. 2, pp. 145–164, 1993.